TEMEL-ij
Technology | Engineering | Management | Entrepreneurship | Learning | International Journal

STUDY OF PHYSICAL PROCESSES IN OPTICAL SYSTEM FOR ELECTRON BEAM WELDING

Assoc. Prof. PhD M. Tongov[1], Prof. Dr.Sc PhD Peter Petrov[2]

Abstract: *This study represents results from mathematical modelling of the electron beam formation into electrostatic field, created by electron optic system (EOS) of the electron beam welding (EBW) gun. Using Finite Element Method (FEM), electrical, thermal and electrostatic tasks are solved. Because of the numerical simulation, the dependences between input (cathode heating current, anode and wehnelt voltage) and beam parameters (current magnitude, spatial arrangement of the crossover and the area of the electron beam) are calculated.*
The structure of the electrostatic field is presented according to the voltage of the anode and wehnelt. The shape and dimensions of the electron beam are determined in the various sections of the electrostatic optic system.

Key words*: **EBW, Electron Beam Welding, Electron Optic System, modelling, numerical simulation***

1. INTRODUCTION

Welding of metals and their alloys takes place because of the introduction and thermodynamic irreversible transformation of one kind of energy into another [1, 2]. In the case of electron beam welding (EBW), the kinetic energy of accelerated electrons into beam is transformed to thermal.
The main advantage of EBW over conventional methods (MMA, MIG/MAG, TIG and plasma welding) is that the thermal source is a highly concentrated energy stream (CES) with high density of power flux into interaction zone between the focused electron beam and the welding sample. This causes a few times the smaller energy, which is introduced into the welding zone, and, consequently, significantly lower influence into heat affected zone (HAZ) and the weld. In welds with large thickness a "dagger" shape is obtained. The processes of EBW and laser welding are highly automated and typically with high welding speed. The ratio between the width b and the weld penetration (h) reaches 1:30 and above (Fig.1). The power density q [W/cm^2] and the welding speed v [cm/s] determine the shape and dimensions of the welds.
Power density is a basic parameter defined as the maximum value of the beam power in a XY plane perpendicular to its axis. The process of electron beam welding with the key-hole formation into the liquid weld pool is possible when power density is greater than it's critical power value P_{cr}, [3,4]. The electron beam area with the power density greater than P_{cr} is defined in [4] as the active zone. For an axisymmetric electron beam, the active zone dimensions (electron beam diameter d_1 and length L_a) are determined by the conditions:

[1] Assoc. Prof. M. Tongov, PhD, Deputy Dean of Faculty of Industrial Technology – TU-Sofia, email: tongov@tu-sofia.bg
[2] Prof. Peter Petrov, Dr.Sc, PhD, Deputy Director Head Laboratory "Physical Technologies, Sliven" Institute of Electronics, BAS, email: peterpitiv@gmail.com

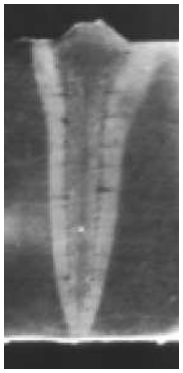

Fig.1. Cross section of the weld (U_a=60[kV]; q=3[kW] and v=1[cm/s]

$$P(r,0,z) \geq P_{cr} \quad (1)$$

$$P(0,0,z) = P_{cr} \quad (2)$$

In [5] has been shown that the quality of the weld is determined by the shape and position of the active zone relative to the welded sample. The parameters of the electron beam active zone are dependent on the design of the electron beam gun (EBG) electrostatic part and characteristics (current density, electron flow density and electron velocity field) formed into it.

In this study, using the numerical modelling methods, the processes in the electrostatic part of the EBG and the formation of the electron beam are described.

2. ELECTRON BEAM GUN

For the numerical experiments an EBG with electrostatic part shown in Fig.2 (cathode node, control electrode (wehnelt) and anode) is considered [6,7]. In ours study, geometry of a real-life EBG is used which has a different configuration and dimensions of the wehnelt and anode (Fig. 3)[8]. The cathode is a band with thickness of 0.1 [mm] and active surface size of 2x2 [mm].

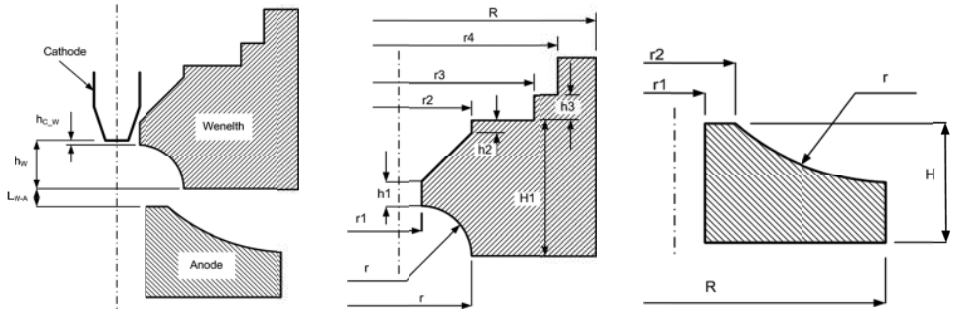

a) b) c)

Fig.2. Common schematic (a), wehnelt (b) and anode (c) parameterized dimensions.

3. SIMULATION MODELLING

Electrons are emitted from the cathode surface. The Richardson law describes the thermionic emission process. According to this equation, the current density of the emission is defined as:

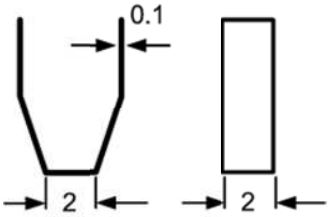

Fig.3. Cathode dimensions

$$j_R = \beta A T^2 \exp\left(-\frac{\varphi}{kT}\right) \quad (3)$$

where β is the material coefficient (for pure tungsten – 0.5 [12]); T - thermodynamic temperature; k - Boltzmann constant; φ - work function (for tungsten φ=4.3[eV]); A - quantum coefficient defined as $A = \left(4\pi m_e k^2 e\right)/h^3$. Here m_e and e are electron mass and charge respectively; h - Plank constant. Under the EBW conditions, the electric field E in front of the cathode may have significant values. Therefore, in this case it is necessary to take into account the Schottky effect. According of this effect the electric field component, normal to surface (E_n) leads to a reduction in the work function with a magnitude:

$$\Delta\varphi = \sqrt{\frac{e^3 E_n}{4\pi\varepsilon_0}}$$

and equation (3) can be written as follows

$$j_{R-S} = \beta A T^2 \exp\left(-\frac{\varphi}{kT}\right).\exp\left(\frac{1}{kT}\sqrt{\frac{e^3 E_n}{4\pi\varepsilon_0}}\right) \quad (4)$$

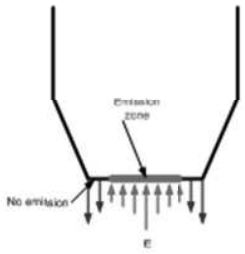

Fig.4. Emission zone on the cathode active surface

The electric field in front of the cathode surface depends on the geometry of the electrostatic part, anode and wehnelt voltage. The anode voltage is positive with respect to the cathode and contributes to the emission and the wehnelt voltage is negative with respect to the cathode and prevents this emission. In the formation of the electron beam, electrons are emitted only those areas of the cathode for which the component of the electric field on the normal to the cathode surface is directed to the cathode (Fig. 4).

It is also possible to emit from other parts of the cathode, but these electrons fall into an electrostatic field, which returns them to the cathode. In fact, some of these electrons, which are emitted near the equipotent surface $E_n = 0$ and have an appropriate orientation of the velocity vector, can enter the field with an anode-accelerating electric field. We do not take this into account. At the same time, we do not take into account the volumetric charge of the electrons in the beam. Its influence is greatest in this area. Thus, the two phenomena are partly offset.

Once the electrons fall into the space between the cathode and the anode they are accelerated by the electrostatic field. The velocity vector has three components - axial, radial and orbital, the latter being the result of the axisymmetric deviation. The radial component leads to the formation of the electrostatic focus (crossover), and the axial one has the main merit of electron energy at the anode outlet. Thus, for the simulation modelling of beam formation, it is necessary to determine the surface temperature of the cathode and the electric field in the space between the cathode, wehnelt and anode.

In the case in question, the cathode is directly heated (by running current). To model these processes the tasks to be solved are: electrical and thermal into the cathode and cathode node; electrostatic and motion (of electrons) into the space between the cathode and the anode. To solve the thermal task in the cathode node (Fig. 5), the differential equation of the heat conduction is used, and for the electric one the equations for the potential and the density of the current in the conducting medium. Since the parameters defining the process do not change over time, the task is resolved as a stationary one. The system of equations is as follows:

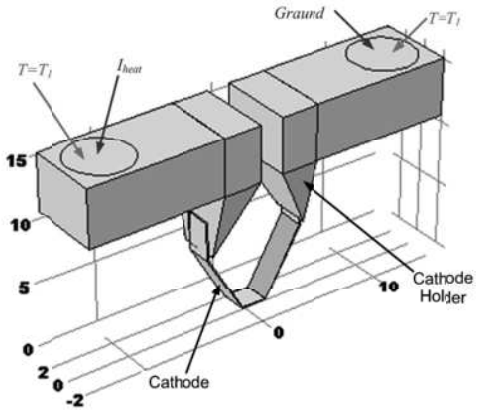

Fig.5

$$\nabla.(\lambda\nabla T) + \frac{j^2}{\sigma} = 0$$
$$\nabla.(\sigma\nabla V_1) = 0 \quad (5)$$
$$\mathbf{j} = \sigma\mathbf{E}_1 \quad \mathbf{E}_1 = -\nabla V_1$$

Here T is the temperature; λ - thermal conductivity (Fig.6); V_1 and $\boldsymbol{E_1}$ - respectively the potential and electric field; σ - the electrical conductivity (Fig.7) and $\boldsymbol{j}$ - the current density.

For the electrical task, the boundary conditions define a zero potential of one of the two current-carrying surfaces, and the other - the heating current. All other surfaces are electrically insulated. The thermal task of these two surfaces is set to the temperature (80°C) because all the current-carrying elements are water-cooled. Part of the cathode carrier is flooded

with polymer. These surfaces that fall into the polymer are set as adiabatic boundaries. For the remaining surfaces, heat removal is prescribed by Stefan-Boltzmann's law. The data used for the emissivity are given in Fig. 8. In addition, the cathode's active surface is assigned a heat output because of the emission of electrons with a heat flux density:

$$q_{emi} = (\varphi - \Delta\varphi).j_{R-S} \tag{6}$$

and

$$j_{R-S} = \begin{cases} \beta A T^2 \exp\left(-\frac{\varphi}{kT}\right).\exp\left(\frac{1}{kT}\sqrt{\frac{e^3 E_n}{4\pi\varepsilon_0}}\right) & E_n \geq 0 \\ 0 & E_n < 0 \end{cases} \tag{7}$$

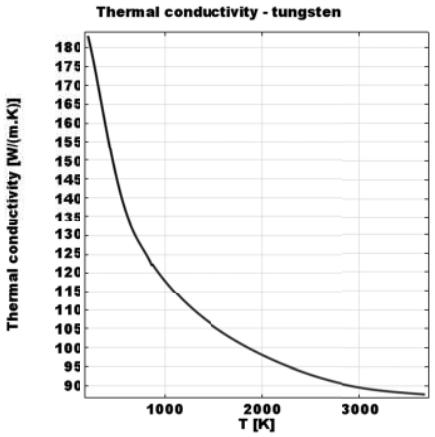

Fig.6

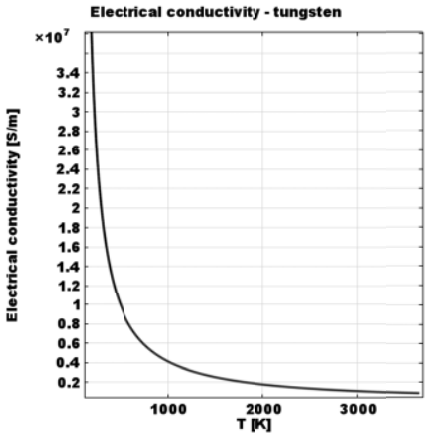

Fig.7

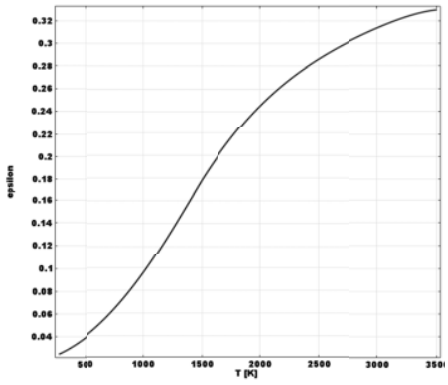

Fig.8. Emissivity of tungsten vs. temperature

In the cathode-cathode carrier contact areas are defined electrical and thermal contact resistors. They are specified for roughness of the contact surfaces 10 μm and the force and the pressing area are determined depending on the actual screw M2. They are defined because they lead to a more even distribution of the temperature on the active surface - the heat removal from the cathode decreases as a result of the heat resistance and the release of heat in the contact electrical resistance.

In the space outside the cathode node, wehnelt and anode (vacuum), the electrostatic field is determined and a task for electron's trajectories is solved. The electrostatic task is solved as a stationary and in fact comes down to a potential task. The equations used are as follows:

$$\nabla^2 V = 0 \quad \mathbf{E} = -\nabla V \tag{8}$$

under the following boundary conditions: all surfaces electrically connected to the cathode have zero potential; the outer surface of the anode and the control electrode have potentials U_a and U_w respectively (U_w <0), with V and $\boldsymbol{E}$ are the potential and electrostatic field respectively.

To model the electron movement in the electrostatic field, a time dependant task is solved and the following equation is used for each electron in the electron beam:

$$\frac{d\left(m_{er}\mathbf{v}_i\right)}{dt} = \mathbf{F}_i$$
$$m_{er} = \frac{m_e}{\sqrt{1-\mathbf{v}_i.\mathbf{v}_i/c^2}} \quad (9)$$

Here m_{er} is the relativistic mass of the electron, $\boldsymbol{F_i}$ is the force it acts on, v_i is electron speed and c is the light speed. This force has two components - one is the result of the interaction with the electrostatic field and the second as a result of the electron - electron interaction under Coulomb's law. This is how it gets

$$\mathbf{F}_i = -e\mathbf{E} - \frac{e^2}{4\pi\varepsilon_0}\sum_{\substack{j=1\\ j\neq i}}^{N}\frac{\mathbf{r}_i - \mathbf{r}_j}{\left|\mathbf{r}_i - \mathbf{r}_j\right|^3} \quad (10)$$

In solving this task, the emission of electron portions from the cathode is generated. Their initial spatial distribution is obtained by dividing the surface of the cathode into a number of areas of approximately the same area (e.g., through the generated finite elements mesh). The number of electrons generated in each area is proportional to the density of the emitted current.

4. RESULTS AND DISCUSSION

The factors that influence the quality of the beam in terms of physical processes are: the temperature distribution on the cathode active surface; the shape and dimensions of the spot in which the electrons are emitted; the structure of the electrostatic field that defines the beam section in the electrostatic focus and the anode outlet; the electron velocity components (axial, radial and orbital) of the anode outlet. In addition, the EBG control characteristic data is important - the beam's current dependence on the wehnelt voltage at different values of the heating current and the anode voltage. For the temperature uniformity of the cathode active surface, the maximum and average temperature graphs can be judged (Fig. 9). It is seen that they practically coincide, which speaks of an even distribution of temperature on this surface. With a given geometry and anode voltage, the emission spot is determined by the voltage of the control electrode. For $L_{W\text{-}A}$ = 7 [mm] and U_A = 50 [kV] it is shown in Fig. 10 (at U_W = -1150 [V] the cathode does not emit). From the result shown, it can be concluded that the voltage of the control electrode must be in the range (-1150, 750) [V]. By lowering this voltage, the shape of the emission spot strives for a circle.

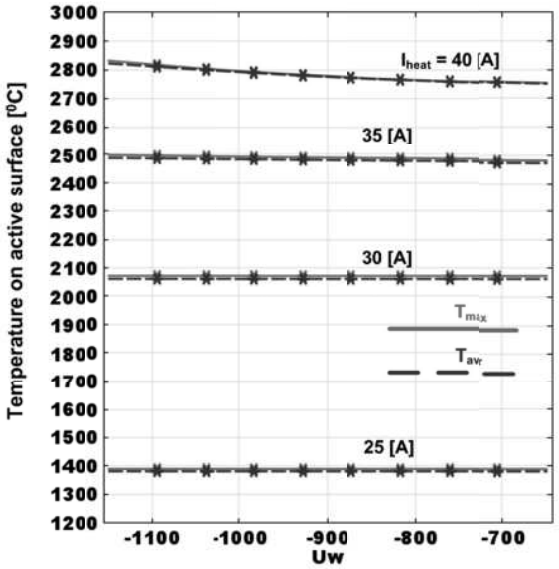

Fig.9. Maximum and average temperature of the active surface depending on the wehnelt voltage at different heating currents and anode voltage 50 [KV].

The axial component of the electrostatic field is responsible for electron accelerating. Fig.11 shows how it changes from the cathode to anode along the symmetry axis and at a distance of 1 [mm] from it (at the end of the active region) (Fig.12) for different control voltage values. These graphs show that a field difference is about the maximum that is located directly in front of the anode and in the cathode region (Fig.13). The last figure shows that U_w = -1150 [V] is the voltage at which the cathode clogs. The distribution of the intensity of the electrostatic field (axial component) in the cathode region is shown in Fig.14. It also shows here that the emitting spot does not cover the entire active surface of the cathode.

Besides the axial strength of the electrostatic field, there are radial and orbital components. Due to the axisymmetric anode and control electrode, the orbital component has no significant value in the electron beam area. At the same time, the radial component is crucial to crossover formation. It can be determined in

the following way (Fig. 15):

$$E_r = E_x \cos(\alpha) + E_y \sin(\alpha) \tag{11}$$

U_W = -650[V] U_W = -750[V] U_W = -850[V] U_W = -950[V] U_W = -1050[V]

Fig.10. Shape and dimensions of the emission spot on the active surface (2x2[mm]).

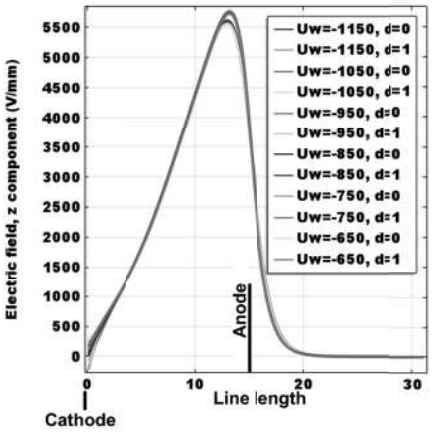

Fig.11

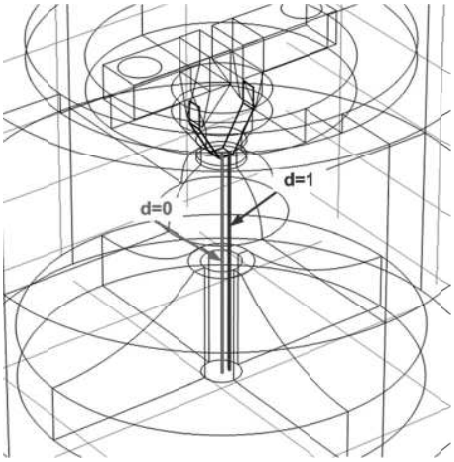

Fig.12.

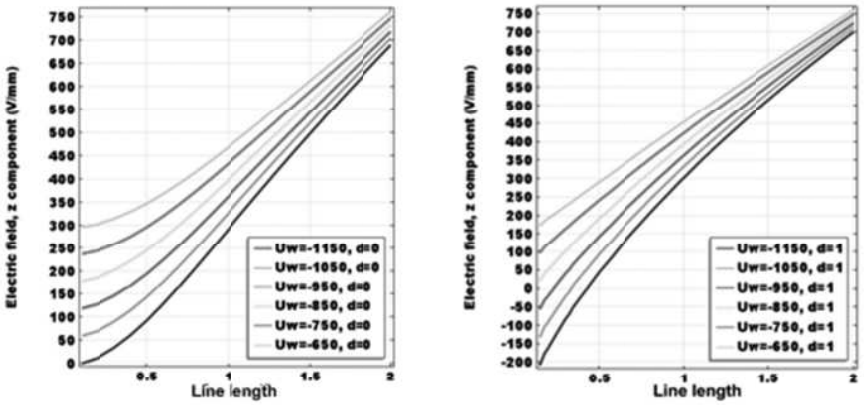

Fig.13. Electric field in front of cathode

The result of the calculation is shown in Fig.16. At positive values of the radial component of the electrostatic field, the forces acting on the electrons are centripetal. Thus, the structure of the electrostatic field in this case is such that when the electrons approach the anode, conditions are created to increase the beam diameter. This type of structure is preserved at all control voltage values.

The magnitude of the electron beam current depends on the heating current, the control electrode voltage and the anode voltage (Fig.17). It is determined by integrating the emitted current density on the cathode active surface:

$$I_{beam} = \int_{S_{active}} j_{R-S}(T, E_n) dS \tag{12}$$

In calculating this integral, the current density is determined in accordance with equation (7). This graph shows that beam current over a wide range can be set in the 35 to 40 [A] range for the heater current.

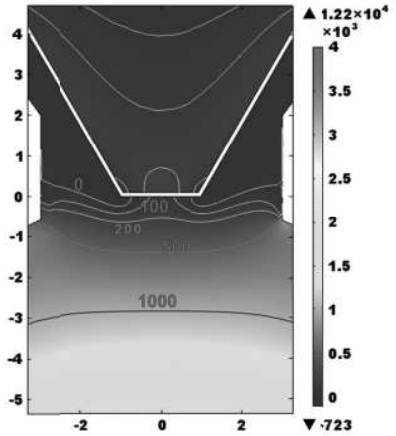

Fig.14. Electric field (electrostatic task)

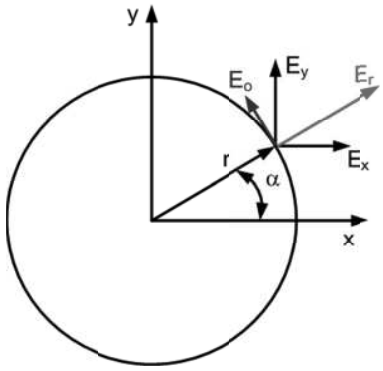

Fig.15. Determination of the radial component of the electric field

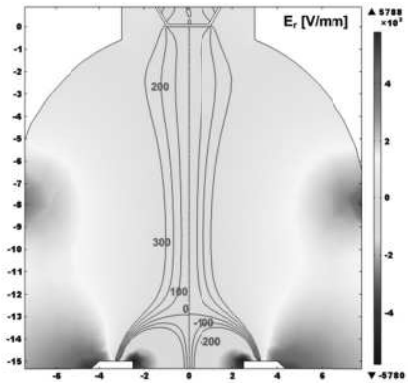

Fig.16. Structure of the electrostatic field

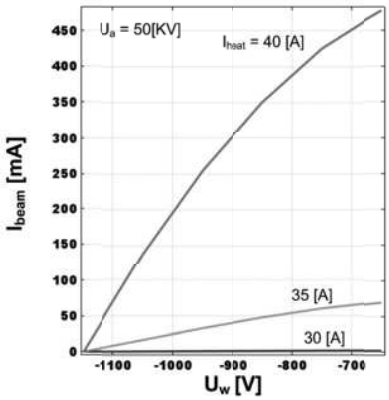

Fig.17. Beam current dependence of the control voltage at different values of the heating current

Beam formation is only tracked for heating current 35 [A]. The overall shape of the beam at the control voltage -650 [V] is shown in Fig.18. The electrostatic focus is visible and in the section of the anode outlet, the shape of the beam is not a circle. In Table 1 and Fig. 18 are given the results for the position of the crossover and its distance from the cathode (δ) for different control voltages. The shape of the beam is represented by the areas through which it passes into three sections: the cathode active surface (black) in the crossover (blue) and the anode outlet (red). By increasing the absolute value of the wehnelt voltage, the crossover approaches the cathode and the beam cross section is retained in the crossover and decreases in the other two considered planes. When the control voltage becomes less than -950 [V], the beam section at the exit of the anode is less than the emission spot on the cathode active surface.

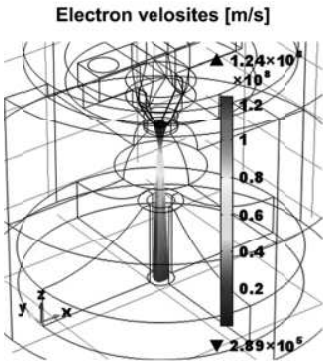

Fig.18. The overall shape of the beam.

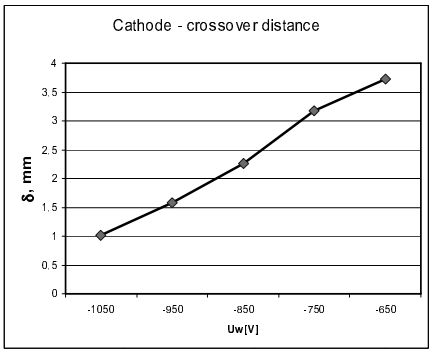

Fig.19. Distance between cathode and crossover.

Table 1.

Crossover position and beam form for different wehnelt voltage.

U_W, [V]	Crossover position	Beam form
-650	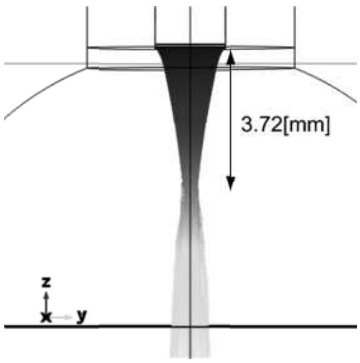	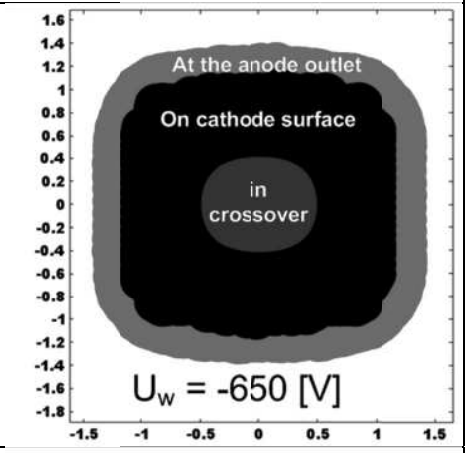
-750	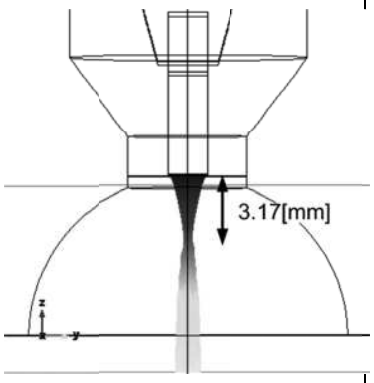	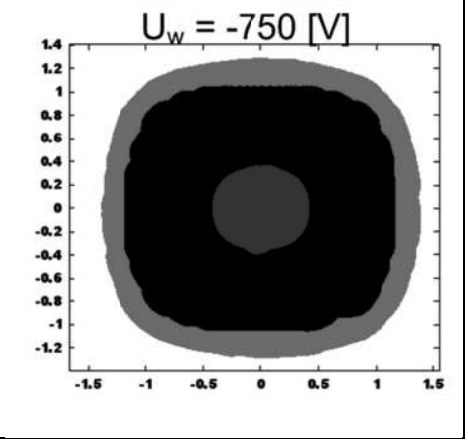

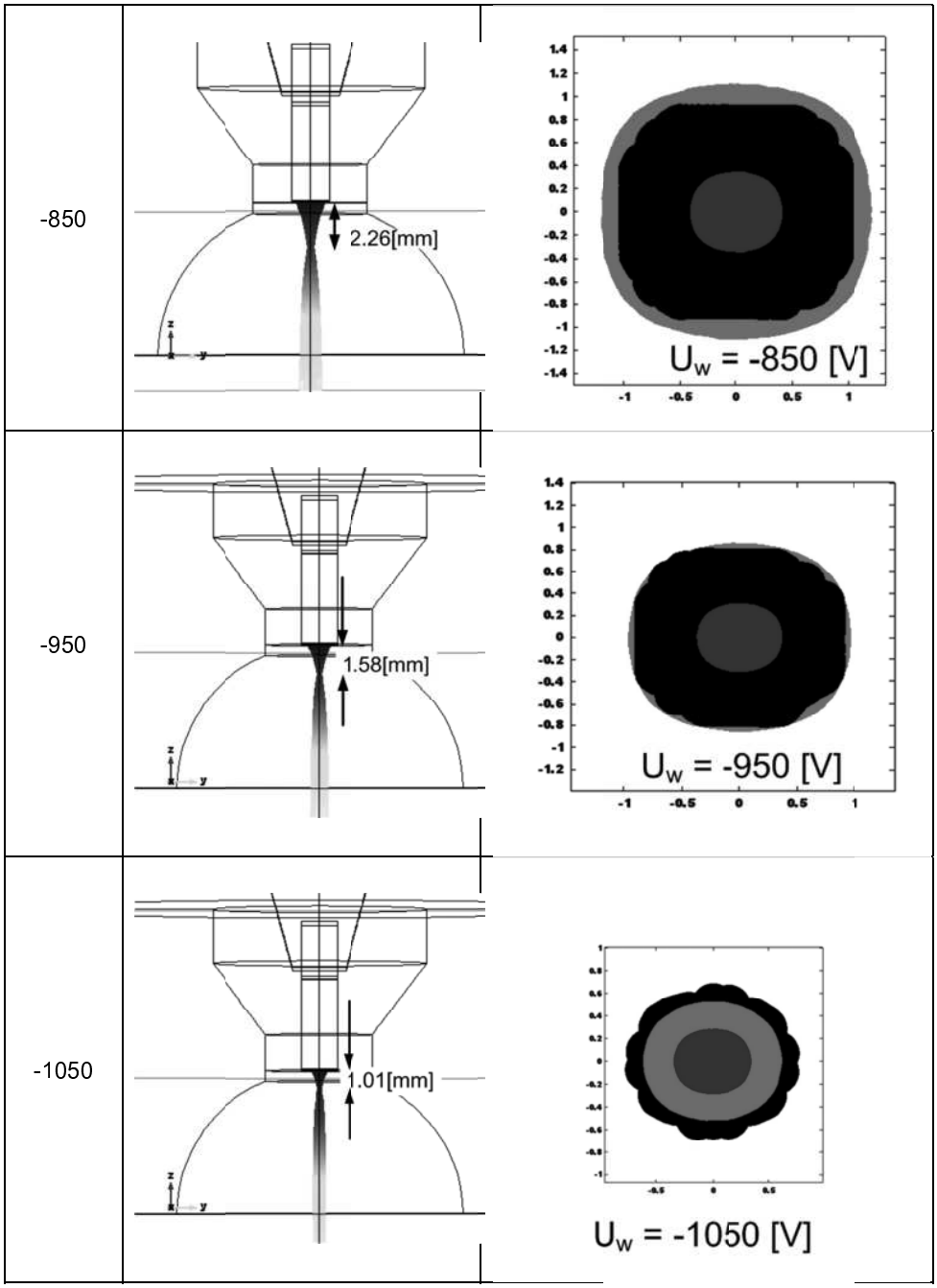

The conclusions reached relate only to the case under consideration and cannot be said to be of a universal nature that is geometrically attached to a particular installation for EBW. The main conclusions that can be drawn are the following.

1. A simulation model of the physical processes in the electrostatic part of the EBG was developed, including the solving of electrical and thermal tasks in the cathode node and electrostatic and the task of moving the electrons in the space between the cathode, wehnelt and anode.

2. By solving the model, using FEM, it was found that the temperature of the active surface is constant at a given heating current (the temperature gradients are negligible). The main reason for this is the cooling effect of the emitted electrons - as the temperature increases, the emission increases as a result of which the heat dissipation increases (there is a self-regulating effect).

3. In the electron emission model the Richardson equation with Schottky correction and material factor for tungsten was used.

4. It has been found that the intensity of the electrostatic field in the axial direction passes through a maximum that is located near the anode. This magnitude is slightly dependent on the control voltage, and only in the area of the maximum and in the immediate vicinity of the cathode.

5. The radial component of the electrostatic field is positive from the surface of the cathode to the maximum indicated, and in this area creates a force aimed at focusing the beam, and in the vicinity of the anode the sign is changed and the force acts defocusing.

6. Adjustment characteristics are shown - the beam current depends on the heating current and the control voltage.

7. It has been found that by increasing the absolute value of the control voltage the distance between the cathode and the crossover decreases. It also reduces the beam section at the anode outlet, this reduction being greater than the reduction of the spot through which the electron emission is realized. This indicates that the reason is not only reducing the magnitude of the beam current. At the same time, the beam size in the crossover does not change.

REFERENCES

[1] S. David, T. Debroy, Science, Vol.257(1992)497.
[2] S. Kou “Welding Metallurgy” A John Wiley&Sons, Inc.Publication,(2002)460p.
[3] Н. Н. Рикалин, А. А. Углов, А. Г. Зуев “Основы электроннолучевой обработки материалов”, Москва, Машиностроене, (1978)238с.
[4] Y.Arata “Plasma, Electron and Laser Beam Technology” American Society for Metals,(1986)630p.
[5] Y. Arata, K. Terai, S. Matsuda, Trans. of JWRI, Vol. 2, n.1(1973)103.
[6] S. Shiller U. Heisig, S. Panzer ”Elektronenstrahltechnologie” Forschungsinstitut Manfred von Ardene, Dresden, VEB Verlag Technik, (1972)528p
[7] Adam, V. et al.: Elektronenstrahlschweißen. pro-beam AG & Co. KgaA, München (2011).
[8] Petrov P., Sabchevski S. “ Parameters used for electron beam welding - A comparative study” Proc. 8th Int. Conf. Beam Technology, Halle, pp. 92-94, (2010).
[9] M. Dulău, L. David, Modeling and simulation of electron’s trajectory inside of electron beam gun, CEAI, Vol. 9, No. 1, pp. 27-32, 2007
[10[A. V. Shcherbakov, M. V. Ivashchenko, A. S. Kozhechenko, and M. S. Gribkov, Parametric Analysis in the Design of Technological Electron Beam Guns, ISSN 10683712, Russian Electrical Engineering, 2016, Vol. 87, No. 1, pp. 41–45. © Allerton Press, Inc., 2016.
[11] E. Lassner, W. Schubert, Tungsten Properties, Chemistry, Jechnology of the Element, Alloys, and Chemical Compaunds, ISBN 978-1-4613-7225-7, Springer Science+Business Media New York, 1999
[12] Кузнецов М. С., Технология получения высокоэмиссионных материалов на основе гексаборида лантана в режиме самораспространяющегося высокотемпературного синтеза при механоактивации шихты, Диссертация на соискание ученой степени кандидата технических наук, 2016

Acknowledgements:
This study was made possible by project ДН 07/26